





## RESEARCH ARTICLE

# Aberrant dynamic structure–function relationship of rich-club organization in treatment-naïve newly diagnosed juvenile myoclonic epilepsy

Guangyao Liu<sup>1,2</sup>  | Weihao Zheng<sup>3</sup>  | Hong Liu<sup>1,2</sup> | Man Guo<sup>3</sup> |  
Laiyang Ma<sup>1,2</sup> | Wanjun Hu<sup>1,2</sup> | Ming Ke<sup>4</sup> | Yu Sun<sup>5,6</sup>  | Jing Zhang<sup>1,2</sup> |  
Zhe Zhang<sup>5,7</sup> 

<sup>1</sup>Department of Magnetic Resonance, Lanzhou University Second Hospital, Lanzhou, China

<sup>2</sup>Gansu Province Clinical Research Center for Functional and Molecular Imaging, Lanzhou, China

<sup>3</sup>Gansu Provincial Key Laboratory of Wearable Computing, School of Information Science and Engineering, Lanzhou University, Lanzhou, China

<sup>4</sup>College of Computer and Communication, Lanzhou University of Technology, Lanzhou, China

<sup>5</sup>Key Laboratory for Biomedical Engineering of Ministry of Education, Department of Biomedical Engineering, Zhejiang University, Hangzhou, China

<sup>6</sup>Zhejiang Lab, Hangzhou, China

<sup>7</sup>School of Physics, Hangzhou Normal University, Hangzhou, China

## Correspondence

Yu Sun, Key Laboratory for Biomedical Engineering of Ministry of Education, Department of Biomedical Engineering, Zhejiang University, Hangzhou, China.  
Email: [yusun@zju.edu.cn](mailto:yusun@zju.edu.cn)

Jing Zhang, Department of Magnetic Resonance, Lanzhou University Second Hospital, Lanzhou, China.  
Email: [lztong2001@163.com](mailto:lztong2001@163.com)

Zhe Zhang, Key Laboratory for Biomedical Engineering of Ministry of Education, Department of Biomedical Engineering, Zhejiang University, Hangzhou, China.  
Email: [zzhang19@zju.edu.cn](mailto:zzhang19@zju.edu.cn)

## Funding information

National Natural Science Foundation of China, Grant/Award Numbers: 61966023, 81801785, 82160326, 82172056

## Abstract

Neuroimaging studies have shown that juvenile myoclonic epilepsy (JME) is characterized by impaired brain networks. However, few studies have investigated the potential disruptions in rich-club organization—a core feature of the brain networks. Moreover, it is unclear how structure–function relationships dynamically change over time in JME. Here, we quantify the anatomical rich-club organization and dynamic structural and functional connectivity (SC–FC) coupling in 47 treatment-naïve newly diagnosed patients with JME and 40 matched healthy controls. Dynamic functional network efficiency and its association with SC–FC coupling were also calculated to examine the supporting of structure–function relationship to brain information transfer. The results showed that the anatomical rich-club organization was disrupted in the patient group, along with decreased connectivity strength among rich-club hub nodes. Furthermore, reduced SC–FC coupling in rich-club organization of the patients was found in two functionally independent dynamic states, that is the functional segregation state (State 1) and the strong somatomotor-cognitive control interaction state (State 5); and the latter was significantly associated with disease severity. In addition, the relationships between SC–FC coupling of hub nodes connections and functional network efficiency in State 1 were found to be absent in patients. The

Guangyao Liu and Weihao Zheng contributed equally to this study.

This is an open access article under the terms of the [Creative Commons Attribution-NonCommercial-NoDerivs](https://creativecommons.org/licenses/by-nc-nd/4.0/) License, which permits use and distribution in any medium, provided the original work is properly cited, the use is non-commercial and no modifications or adaptations are made.

© 2022 The Authors. *Human Brain Mapping* published by Wiley Periodicals LLC.

aberrant dynamic SC–FC coupling of rich-club organization suggests a selective influence of densely interconnected network core in patients with JME at the early phase of the disease, offering new insights and potential biomarkers into the underlying neurodevelopmental basis of behavioral and cognitive impairments observed in JME.

#### KEYWORDS

brain networks, dynamic SC–FC coupling, juvenile myoclonic epilepsy, rich-club organization, treatment-naïve

## 1 | INTRODUCTION

Juvenile myoclonic epilepsy (JME) is the most common generalized genetic epilepsy syndrome, accounting for up to 10% of all epilepsies (Camfield, Striano, & Camfield, 2013; Scheffer et al., 2017). The syndrome's clinical characteristics include myoclonic jerks, tonic–clonic seizures, and less frequent absence seizures, with typically cognitive deficits in working memory, attention, and executive functions (Carvalho et al., 2016; Pascualichio et al., 2007; Wandschneider, Thompson, Vollmar, & Koepp, 2012). Although the underlying neural substrates for JME remain elusive, recent neuroimaging studies have provided ample evidence of both abnormal structural connectivity (SC) and functional connectivity (FC) in the connectome of patients (Caeyenberghs et al., 2015; Jiang et al., 2018; Ur Ozcelik et al., 2021; Zhong et al., 2018), together with disrupted topological organization (Parsons, Bowden, Vogrin, & D'Souza, 2020). These prior research has conceptualized JME as a disorder of brain network dysfunction, providing a new insight for understanding the underlying pathophysiology and etiology of this disorder.

A prominent feature of the brain networks is the rich-club organization, which describes a set of highly central and interconnected anatomical hub regions (van den Heuvel & Sporns, 2011). Generally, the rich-club organization forms a central structural backbone for global brain communication and thus plays a crucial role in integrating functional control and information flow (van den Heuvel, Kahn, Goni, & Sporns, 2012). Disrupted rich-club organization has been repeatedly reported in previous studies of neuropsychiatric disorders, such as schizophrenia (van den Heuvel et al., 2013), attention-deficit hyperactivity disorder (Ray et al., 2014), autism spectrum disorder (Keown et al., 2017), major depressive disorder (X. Liu et al., 2021), and generalized tonic–clonic seizures (Li et al., 2016), indicating that rich-club disorganization may have a key role in the etiology of these disorders. However, it remains largely unknown how anatomical rich-club organization changes in JME.

Moreover, it is widely known that the structural connections shapes and constrains the function of nervous systems in multiple scales. Studies using multimodal MRI techniques have also demonstrated the spatial correspondence between structural and functional brain networks (Misić et al., 2016), thereby providing important information about how structural constraint supports functional communication. The relationship between SC and FC profiles, namely SC–FC

coupling, characterizes the functional dynamics of structural topological properties (Grayson et al., 2014; Zhao et al., 2020), which is prominently associated with the higher-order cognitive processes such as executive function (Baum et al., 2020; Suarez, Markello, Betzel, & Misić, 2020; van den Heuvel et al., 2013). Atypical development of SC–FC coupling could contribute to the emergence of neuropsychiatric disorders such as JME (Jia et al., 2018). Of note, the abovementioned studies on SC–FC coupling assume that the FC between two brain regions remains constant throughout the entire MRI scan. In fact, the human brain is known to be highly dynamic (Calhoun, Miller, Pearlson, & Adali, 2014). Hence, the dynamic FC, which describes the time-varying patterns of co-activations among brain regions, is a more efficient way for uncovering specific properties of functional communication in health and disease (Allen et al., 2014; Calhoun & Adali, 2016; Fiorenzato et al., 2019; F. Liu et al., 2017; Sun, Collinson, Suckling, & Sim, 2019; Tu et al., 2020). For patients with JME, previous studies have revealed that the dynamic FC was reduced and linked to disease severity (Wang, Berglund, Uppman, & Li, 2019; Zhang et al., 2018, 2020). However, to our knowledge, no prior study has explored the time-varying characteristics of SC–FC coupling in JME, and it is still unclear how anatomical connectivity constraint supports dynamic functional interaction in the rich-club organization.

This study aims to investigate the changes of rich-club organization and its dynamic SC–FC coupling in treatment-naïve newly diagnosed patients with JME. We first examined the differences in the white matter connectivity of rich-club organization between patients and controls. By performing dynamic FC analysis, we then examined the group differences in the SC–FC coupling of rich-club organization in each identified dynamic state (depicting transient FC patterns over time). Moreover, the relationships between SC–FC coupling and dynamic functional network efficiency were calculated to explore the supporting of structure–function coupling to brain information transfer. In addition, we correlated brain changes with clinical measures of patients to understand whether structure–function relationship could be a potential indication for the progress of disease. Based upon the previous evidence supporting impaired brain networks in JME (Parsons et al., 2020; Wang et al., 2019), we hypothesized that: (a) the rich-club organization is disrupted in patients; and (b) the SC–FC coupling and its support to functional network efficiency are altered in some specific dynamic states in patients.

## 2 | MATERIALS AND METHODS

### 2.1 | Participants

Sixty-eight treatment-naïve newly diagnosed patients with JME were recruited from outpatient at the Epilepsy Center of Lanzhou University Second Hospital. All of them fulfilled the epilepsy classification criteria of the International League Against Epilepsy (ILAE) guidelines for JME (Jerome Engel, 2001). Routine MRI scans were normal, and routine scalp EEG showed 3–6 Hz generalized spike-wave or polyspike-wave discharges (GSWDs). Exclusion criteria for patient group were as follows: (a) a history of any forms of antiseizure medication; (b) other neurological or major psychiatric illness; (c) other developmental disabilities, such as autism and intellectual impairment; and (d) acute physical illness that would affect the scanning. The seizure severity of each patient was assessed using the National Hospital Seizure Severity Scale (NHS3), which is a valid, easily applicable measure of seizure severity (O'Donoghue, Duncan, & Sander, 1996). It contains six seizure-related factors (Chinese version), such as generalized convulsions, falls, incontinence, loss of consciousness, duration of recovery time, and automatisms, and generates a total score from 1 to 23. Forty-eight healthy controls were recruited from the local community via advertisement and those with a history of febrile convulsions, seizures, or family history for epilepsy were excluded. This study was approved by the Ethics Committee of Lanzhou University Second Hospital. Written informed consent was obtained from all participants.

After head motion exclusion, the remaining 47 patients and 40 healthy controls were included in the subsequent analyses. Detailed demographic and clinical characteristics of all participants included in this study are shown in Tables 1 and S1. The basic flow of this study is depicted in Figure 1.

### 2.2 | MRI acquisition and data preprocessing

All MRI data were acquired on a Siemens Verio 3.0 T scanner (Siemens, Erlangen, Germany) with a 32-channel head coil at Lanzhou

University Second Hospital. Participants were asked to stay awake with their eyes closed, to remain still, and not to think systematically during the scan. To minimize the head motion, participants' heads were stabilized in the head coil using foam pads. High-resolution structural 3D T1-weighted images were obtained using a magnetization-prepared rapid gradient-echo sequence (repetition time [TR] = 1900 ms; echo time [TE] = 2.99 ms; flip angle = 90°; slice thickness = 0.9 mm; acquisition matrix = 256 × 256; field of view [FOV] = 230 × 230 mm<sup>2</sup>; in-plane resolution = 0.9 × 0.9 mm<sup>2</sup>; and slices = 192). Resting-state functional scans were acquired using an echo-planar imaging sequence (TR = 2000 ms; TE = 30 ms; flip angle = 90°; slice thickness = 4 mm; in-plane matrix resolution = 64 × 64; FOV = 240 × 240 mm<sup>2</sup>; slices = 33; 200 volumes; and a total of 400 s). DWI scans were obtained using a diffusion weighted spin echo EPI sequence (TR = 11,300 ms; TE = 85 ms; flip angle = 90°; NEX = 1; voxel size = 2.0 × 2.0 × 2.0 mm<sup>2</sup>; matrix = 128 × 128; FOV = 256 × 256 mm<sup>2</sup>; thickness = 2 mm without gap; 60 slices covered the whole brain). Three diffusion-weighted volumes were acquired with  $b = 0$  s/mm<sup>2</sup> and 30 diffusion weighted directions with  $b = 1,000$  s/mm<sup>2</sup> and the total scan time was 386 s.

Resting-state fMRI data were preprocessed using the DPARSF toolbox (Yan & Zang, 2010). The main preprocessing steps included discard 10 initial volumes, time-slicing correction, head motion realignment, normalization to the Montreal Neurological Institute (MNI) space, and spatial smoothing using a Gaussian kernel of 6 mm full width at half maximum. To minimize the potential effects of head motion on FC, we excluded the participants with head motion over than 2 mm translation or 2° rotation. We also calculated the mean frame-wise displacement (FD) of each participant on the basis of realignment parameters and excluded the participants with mean FD more than 0.2 mm.

DWI images of each participant were preprocessed using the PANDA toolbox (Cui, Zhong, Xu, He, & Gong, 2013). The main preprocessing included four steps as follows: (1) estimate the brain mask using b0 image; (2) remove nonbrain tissue in the raw images;

**TABLE 1** Demographic and clinical characteristics of all participants

	JME ( $n = 47$ )	HC ( $n = 40$ )	$p$ -Value
Age (years)	17.17 ± 4.12	18.08 ± 3.64	.29 <sup>a</sup>
Gender (males/females)	23/24	13/27	.25 <sup>b</sup>
Handedness (right/left)	47/0	40/0	-
Seizure semiology	MS (47), GTCS (33)	-	-
Age at seizure onset (year)	15.32 ± 2.96	-	-
Duration of epilepsy (months)	21.72 ± 19.22	-	-
NHS3 total score	9.23 ± 3.94	-	-
Mean FD	0.12 ± 0.07	0.12 ± 0.03	.62 <sup>a</sup>

Note: Values are mean ± SD.

Abbreviations: FD, frame-wise displacement; GTCS, generalized tonic-clonic seizure; HC, healthy control; JME, juvenile myoclonic epilepsy; MS, myoclonic seizure; NHS3, the National Hospital Seizure Severity Scale.

<sup>a</sup>Two sample  $t$  test.

<sup>b</sup>Chi-square  $t$  test.

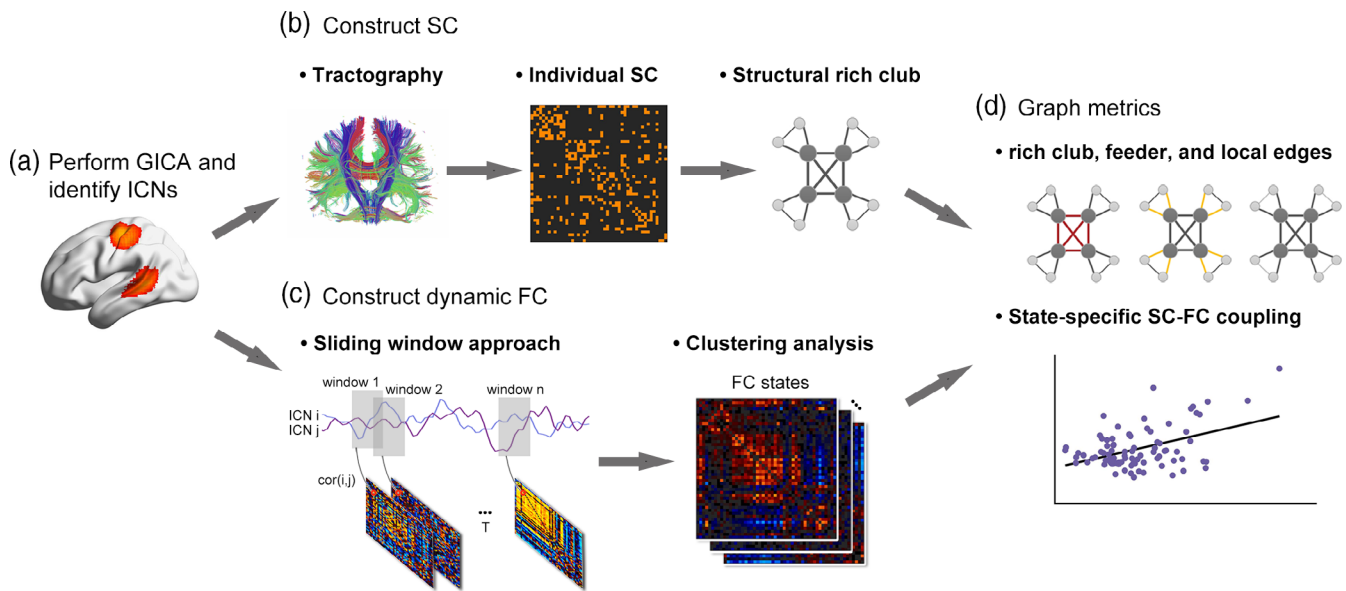


**FIGURE 1** Analysis flowchart to study dynamic structural connectivity and functional connectivity (SC-FC) relationships of rich-club organization in patients with juvenile myoclonic epilepsy (JME). Four major steps were included: (a) perform group independent component analysis (GICA) and select intrinsic connectivity networks (ICNs); (b) construct structural brain networks between ICNs and find anatomical rich-club organization; (c) estimate dynamic functional network connectivity and perform clustering state analysis; and (d) conduct SC-FC coupling analysis based on graph theoretical metrics

(3) corrections for eddy-current distortion and head motion; and (4) calculate the diffusion tensor metrics including fractional anisotropy (FA), mean diffusivity, axial diffusivity, and radial diffusivity maps.

### 2.3 | Group independent component analysis

To identify the intrinsic connectivity networks (ICNs) and their corresponding activation spatial maps, we used a standard pipeline of spatial GICA implemented in the GIFT toolbox (<http://mialab.mrn.org/software/gift/>) to decompose the fMRI data into multiple independent components (ICs). A principal component analysis was first conducted to reduce participant-specific data into 120 principal components. Then, participant-reduced data of all participants across time were concatenated and further reduced into 100 ICs using the infomax algorithm (Bell & Sejnowski, 1995). We selected the ICNs among 100 ICs by a combination of spatial template-matching and visual inspection. Templates were derived from the ICA analyses as described in previous studies (Allen et al., 2014; F. Liu et al., 2017). The ICNs were further evaluated to test if the peak activation coordinates were located primarily in gray matter, low spatial overlap with known artifacts (including vascular, ventricular, motion, and susceptibility artifacts), and time courses were dominated by low-frequency fluctuations (Allen et al., 2014; Fiorenzato et al., 2019). Finally, 47 ICNs were identified and grouped into seven resting-state networks (RSNs) based on the spatial correlation values between ICs and the template (Allen et al., 2014; F. Liu et al., 2017). As shown in Figure 2, these RSNs were arranged into subcortical (SubC; 1 ICNs), auditory (AUD; 3 ICNs), visual (VIS; 8 ICNs), somatomotor (SM;

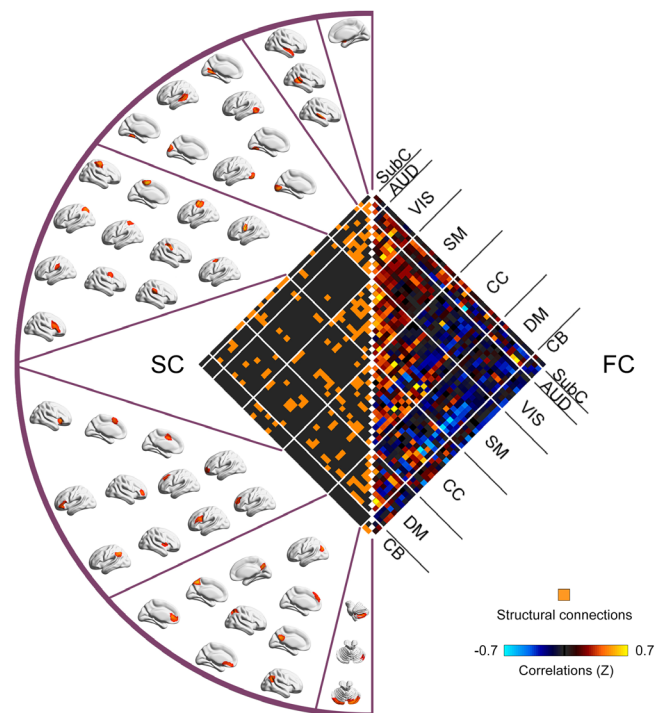


**FIGURE 2** Averaged structural connectivity and static functional connectivity between ICN pairs across all participants. Intrinsic connectivity network (ICN) maps ( $N = 47$ ) were identified by a group independent component analysis (GICA) and grouped into seven resting-state networks based on their anatomical and functional properties, such as subcortical (SubC), auditory (AUD), visual (VIS), somatomotor (SM), cognitive control (CC), default mode (DM), and cerebellar (CB) networks

11 ICNs), cognitive control (CC; 12 ICNs), default mode (DM; 9 ICNs), and cerebellar (CB; 3 ICNs) networks. Detailed information regarding activation spatial maps of these ICNs are provided in Table S2.

## 2.4 | Brain networks construction

### 2.4.1 | Structural brain networks

We defined the 47 ICNs as nodes in the white matter network. The spatial maps of these ICNs in the MNI space were transformed into the native DWI space of each participant. Specifically, the individual FA image in the native space was first co-registered to its b0 image using a linear transformation, and then the b0 image was nonlinearly registered to the ICBM152 template. Based on the resultant transformations in these two steps, an inverse warping transformation from the MNI space to the native DWI space can be obtained. To reconstruct the edges in the white matter network, we tracked the white matter fibers between pairs of ICNs using the deterministic tractography, which has been shown to be a suitable method for reconstructing the connectome (Sarwar, Ramamohanarao, & Zalesky, 2019). In particular, we chose this metric as a measure of the strength of SC since it has been widely used to quantify the anatomical rich-club organization in previous studies (Li et al., 2016; Liu et al., 2021; van den Heuvel et al., 2013; Zhao et al., 2020), which makes our findings be comparable to these studies. Deterministic tractography was performed in the native space for each participant using the fiber assessment by continuous tracking (FACT) algorithm (Mori, Crain, Chacko, & Van Zijl, 1999). Here, fiber tracking was terminated when the angle between two consecutive orientations was  $>45^\circ$  or when the FA value was  $<0.2$ . Given that the outcome of tractography is affected by the initial position of the seed points within the voxel, 100 seeds were randomly selected within each voxel to avoid biases from initial seed positioning. Resultant whole-brain tracts provided the edges for building the white matter network. SC was weighted as the number of deterministic fiber streamlines (FN) connecting each pair of nodes. To further assess the reproducibility of our findings, we have also taken average FA of the streamlines, streamline volume density (SVD; obtained by dividing the FN by the average cortical volume of the connected regions and corrected for potential effects of differences in cortical volume), streamline length density (SLD; obtained by dividing the FN by the mean length of streamlines and compensated for the bias toward longer fibers during streamline reconstruction), and the product of FN and average FA ( $FA \times FN$ ) as weight of SC.

### 2.4.2 | Dynamic functional brain networks

The dynamic functional brain networks were estimated using a sliding window approach and a clustering analysis (Allen et al., 2014). A tapered window was used to divide the time courses of ICNs into 169 windows with one TR increment-step across the entire scan for each participant. Of note, here the window length of 22 TRs was selected, which has been demonstrated to provide a good trade-off

between the quality of the correlation matrix estimation and the ability of to detect functional dynamics (Allen et al., 2014). The covariance matrix with  $47 \times 47$  size within each window was calculated to construct functional brain networks (Smith et al., 2011), wherein each ICN was defined as node and the correlation between two ICNs was defined as an edge. The resulting 169 matrices for each participant represent the dynamic changes of functional brain networks over time. Subsequently, a k-means clustering analysis was conducted on the dynamic FC matrices of all participants to estimate reoccurring functional network connectivity states that represent the transient patterns of FC over time. We categorized these matrices into five distinct clusters based on the similarity of L1 distance between matrices and cluster centroids. The optimal number of clusters was estimated using the elbow criterion, which is defined as the ratio of within cluster distance to between-cluster distance, and each cluster represented a different dynamic state (Damaraju et al., 2014). To verify the reproducibility of the findings across different sliding window sizes and number of clusters, we also constructed the dynamic functional brain networks and tested group differences in the window sizes of 18–26 TRs (36–52 s) and the number of clusters as 4 and 6.

## 2.5 | Graph theoretical metrics

### 2.5.1 | Anatomical rich-club organization

We identified the rich-club organization of the structural brain networks using the approach as described in van den Heuvel et al. (2012). Briefly, the weighted rich-club coefficient  $\varphi^w(k)$  was computed as the ratio between the sum of the weights of the edges' subset with degree  $> k$  and the sum of the weights of all the connections of the whole network. The normalized rich-club coefficient  $\varphi_{\text{norm}}(k)$  was defined as the ratio of  $\varphi^w(k)$  in the structural brain network and the mean  $\varphi_{\text{random}}(k)$  across 1000 random networks. According to the  $\varphi_{\text{norm}}(k)$  for a given  $k$ , rich-club nodes and local nodes were identified for each participant, and the edges associated with these nodes were further categorized into the rich club, feeder, and local edges, representing the connections linking rich-club nodes, linking rich-club nodes and nonrich-club nodes, and linking nonrich-club nodes, respectively. Of note, rich-club nodes were defined on the basis of the group-averaged structural network, which was computed by selecting the connections that were present in at least 75% of all participants.

### 2.5.2 | Dynamical functional network efficiency

To characterize the parallel information transfer in the functional brain networks, we evaluated the network efficiency (defined as inversely proportional to the harmonic mean of the shortest distance between all possible pairs of nodes) for each participant and each dynamic state, both globally (global efficiency) and locally (local efficiency). The network efficiency was calculated at a sparsity threshold  $S$  (the ratio of the number of actual edges to the maximum possible number of

edges in a network). Here, the threshold range of sparsity was identified as 0.1 to 0.35 in 0.01 increments. We applied an area under the curve (AUC) approach to avoid the specific selection of a threshold as suggested by previous studies (Tu et al., 2019; Yu et al., 2015). Finally, the AUC was calculated within the defined threshold range for each measure of network efficiency.

## 2.6 | SC-FC coupling

The level of SC-FC coupling was measured as the Pearson's correlation between the strength of the structural connections and their functional counterparts in each dynamic FC state. Of note, the fiber strengths reconstructed by the streamline tractography are exponentially distributed and spanned several orders of magnitude, yet interregional physiological efficacies would not span such a large range (Honey et al., 2009). Thus, following previous studies (Collin, Scholtens, Kahn, Hillegers, & van den Heuvel, 2017; van den Heuvel et al., 2013; Zhao et al., 2020), these correlations were constrained by the edges with nonzero values in the structural brain networks, which were rescaled to Gaussian distributions before coupling analysis. The SC-FC coupling analysis was performed for the three categories of connections (i.e., rich club, feeder, and local edges) separately, resulting in different types of SC-FC coupling matrices for each of the brain networks.

## 2.7 | Statistical analysis

Group differences in age and gender were explored using a two-sample *t* test and a chi-square test, respectively. Differences in rich-club organization measures and dynamic network efficiency between patients and controls were examined using a Wilcoxon rank test. In addition, the Spearman's correlation analysis was conducted to examine the relationships between altered brain measures and clinical measures (i.e., age at seizure onset, disease duration, presence of generalized tonic-clonic seizure, and NHS3 score) in patients, controlling for age, gender, and mean FD. All statistical analyses were performed by SPSS 24.0 (IBM Corporation, Armonk,

NY). Statistical significance was established at  $p < .05$  with false discovery rate (FDR) correction conducted for each brain measure separately.

## 2.8 | Data availability

The data that support the findings of this study are available from the corresponding author (Zhe Zhang) upon reasonable request.

## 3 | RESULTS

### 3.1 | Anatomical rich-club organization

No significant group differences in the structural network density ( $Z = -.215, p = .728$ ) and overall SC strength ( $Z = -1.192, p = .255$ ) were found. Relative to controls, patients had a lower rich-club coefficient  $\varphi_{\text{norm}}(k)$  for degree  $k$  ranging from 10 to 13 ( $Z = -2.923, p = .006$ ; Figure 3a). Figure 3b shows the rich-club regions in the structural brain network (averaged over participants) for degree  $k > 11$ , including bilateral middle temporal gyrus, precentral gyrus, superior parietal lobule, insula, inferior parietal lobule, and right inferior frontal gyrus. We further investigated the group differences in the strength of three connection categories and found that the density of rich-club edges was significantly decreased in patients when compared with controls ( $Z = -3.100, p = .003$ , FDR-corrected; Figure 3c), suggesting that anatomical rich-club connectivity is selectively affected in patients with JME. These findings were validated in other degrees of rich-club examination ( $k = 10-13$ ). Examining other definitions of SC weight, such as average FA, SVD, SLD, and  $\text{FA} \times \text{FN}$ , showed similar results (see details in Figure S1).

### 3.2 | Dynamic SC-FC coupling

The visualized connectivity patterns (centroids of clusters) of five dynamic FC states across all participants are shown in Figure 4a. We first investigated the FC counterparts of structural connection

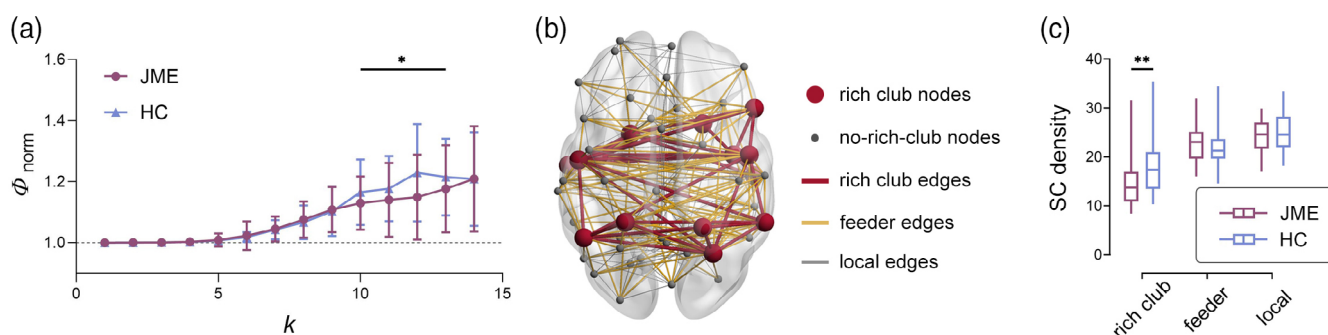


**FIGURE 3** Rich-club organization in the structural brain network. (a) The average  $\varphi_{\text{norm}}(k)$  is plotted against the degree ( $k$ ) for both healthy controls (HCs) and patients with juvenile myoclonic epilepsy (JME). (b) Averaged structural connectivity network for all participants. Rich-club regions (red) were identified by setting the threshold as degree  $> 11$ . (c) Box charts showing mean (SD) density values of rich club, feeder, and local edges per participant group. \* $p < .05$ , \*\* $p < .01$ , FDR-corrected

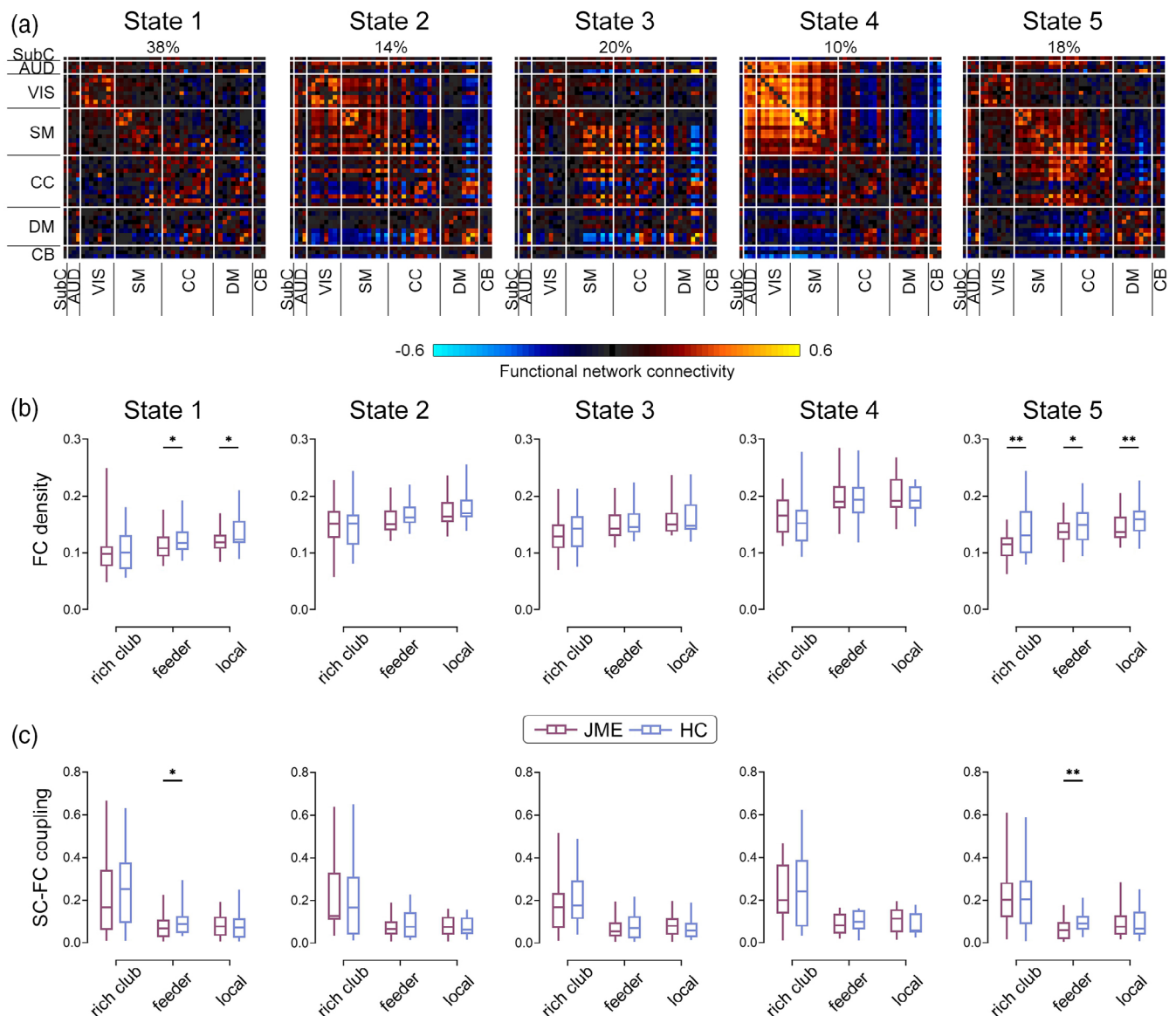


**FIGURE 4** State-specific functional connectivity density and structural connectivity and functional connectivity (SC-FC) coupling of rich-club organization measures. (a) Five discrete dynamic functional connectivity patterns across all groups. (b) Box charts showing mean (SD) density values of FC counterparts of rich club, feeder, and local edges per participant group for each state. (c) Box charts showing mean (SD) level values of SC-FC coupling of rich club, feeder, and local edges per participant group for each state. JME, juvenile myoclonic epilepsy; HC, healthy controls. \* $p < .05$ , \*\* $p < .01$ , FDR-corrected

categories in each dynamic state and compared them between groups. As shown in Figure 4b, patients exhibited a significant decrease in the strength of FC counterpart of rich-club edges in State 5 ( $Z = -3.102$ ,  $p = .003$ , FDR-corrected), as well as in the strength of FC counterparts of feeder and local edges in both State 1 (feeder edges  $Z = -2.612$ ,  $p = .010$ ; local edges  $Z = -2.484$ ,  $p = .013$ , FDR-corrected) and State 5 (feeder edges  $Z = -2.176$ ,  $p = .021$ ; local edges  $Z = -2.871$ ,  $p = .008$ , FDR-corrected). State 1 showed a predominance of within-RSN connections whereas State 5 exhibited strongly positive couplings between the SM and CC. We then explored the SC-FC coupling of every connection category in each state and observed a significant group difference. Specifically, for patients, the level of SC-FC coupling of feeder edges was significantly decreased in both State 1 ( $Z = -2.415$ ,  $p = .016$ , FDR-corrected) and

State 5 ( $Z = -2.792$ ,  $p = .009$ , FDR-corrected; Figure 4c). These findings were independent of different settings of sliding window (Figures S2 and S3) and clusters (Figures S4, S5), indicating JME-related state-specific disruptions of SC-FC coupling in feeder edges.

### 3.3 | Relationship between SC-FC coupling and functional network efficiency

To investigate how structure-function coupling supports information transfer in the functional brain networks, we evaluated dynamic network efficiency and correlated it with the SC-FC coupling of every connection category in each state. We observed that the patients not only showed a lower global efficiency in State 1 ( $Z = -2.866$ ,

$p = .008$ , FDR-corrected; Figure 5a) but also exhibited a lower local efficiency both in State 1 ( $Z = -2.901$ ,  $p = .007$ , FDR-corrected) and State 5 ( $Z = -2.183$ ,  $p = .0201$ , FDR-corrected; Figure 5b). Further observation revealed that the SC-FC coupling of rich-club edges was both significantly correlated with the global efficiency ( $r = -.45$ ,  $p = .005$ , FDR-corrected; Figure 5c) and local efficiency ( $r = -.44$ ,  $p = .006$ , FDR-corrected; Figure 5d) in State 1 in healthy controls, while these relationships were not present in patients. These findings suggest that the constraint of SC-FC coupling to functional network efficiency in specific dynamic state is relaxed in JME.

### 3.4 | Clinical correlates

We further test whether brain network measures with significant group differences are correlated with clinical variables. As shown in Figure 6, we found that the SC-FC coupling of feeder edges in State

5 was negatively correlated with the NHS3 scores in patients ( $r = -.47$ ,  $p = .005$ , FDR-corrected). This means that the lower level of SC-FC coupling in State 5 is associated with the greater disease severity. In addition, we did not find any significant associations between other clinical variables (e.g., age at seizure onset, disease duration, and presence of generalized tonic-clonic seizure) and aberrant SC-FC coupling (all tests  $p > .05$ , FDR-corrected).

## 4 | DISCUSSION

We performed a combination analysis of SC and dynamic FC, for the first time, to examine the abnormalities in the rich-club organization and its dynamic SC-FC coupling in treatment-naïve newly diagnosed JME. Beyond previous studies reporting altered rich-club organization and structure-function coupling in generalized epilepsy, we not only found significant rich-club organization deficits but also state-specific

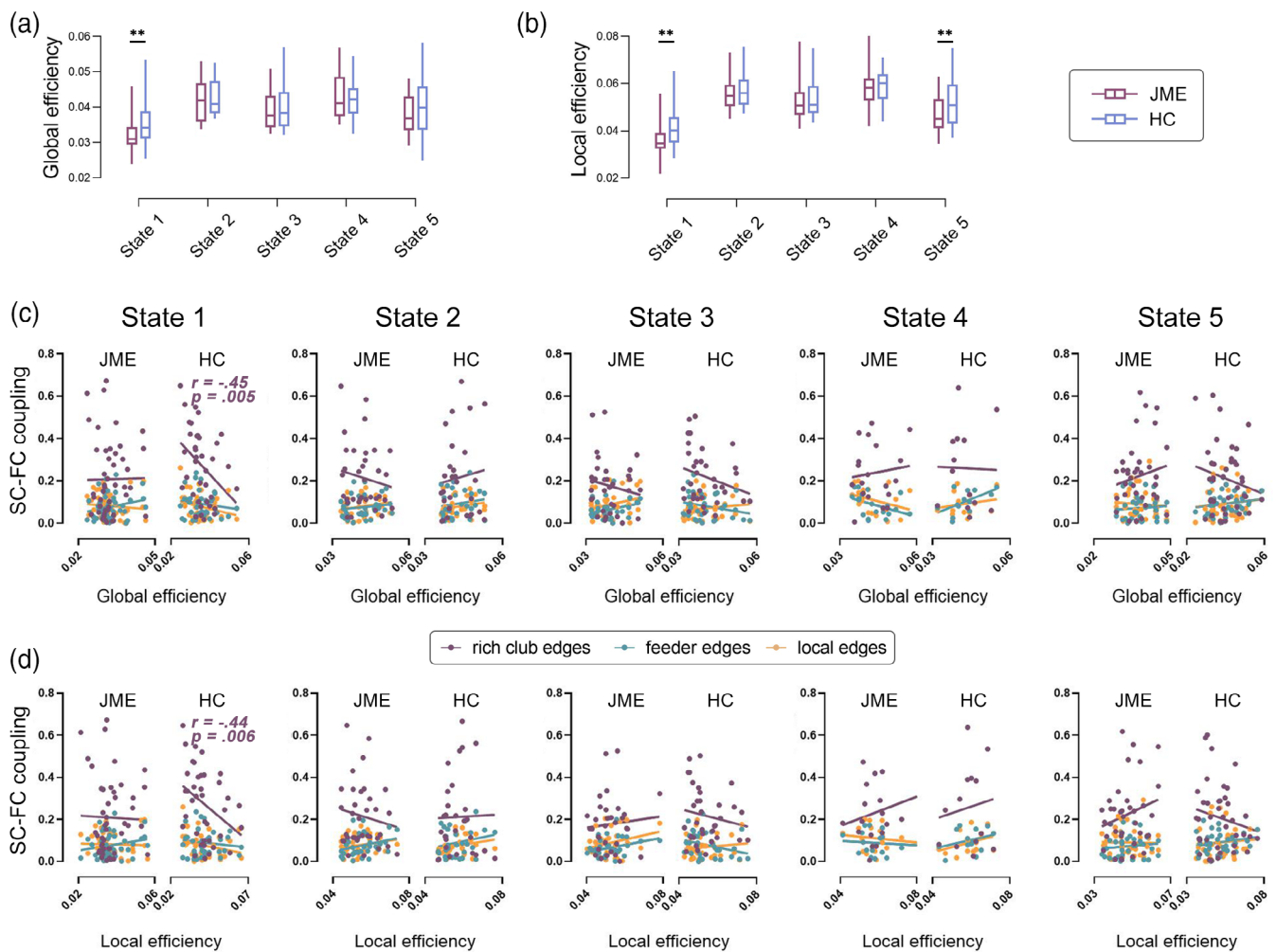


**FIGURE 5** Dynamic network efficiency and its association with structural connectivity and functional connectivity (SC-FC) coupling. (a) Box charts showing mean (SD) values of global efficiency per participant group for each state. (b) Box charts showing mean (SD) values of local efficiency per participant group for each state. (c) Scatter plot showing the association between global efficiency and SC-FC coupling of rich club, feeder, and local edges in patients with juvenile myoclonic epilepsy (JME) and healthy controls (HCs) for each state. (d) Scatter plot showing the association between local efficiency and SC-FC coupling of rich club, feeder, and local edges in patients with JME and HCs for each state.

\* $p < .05$ , \*\* $p < .01$ , FDR-corrected



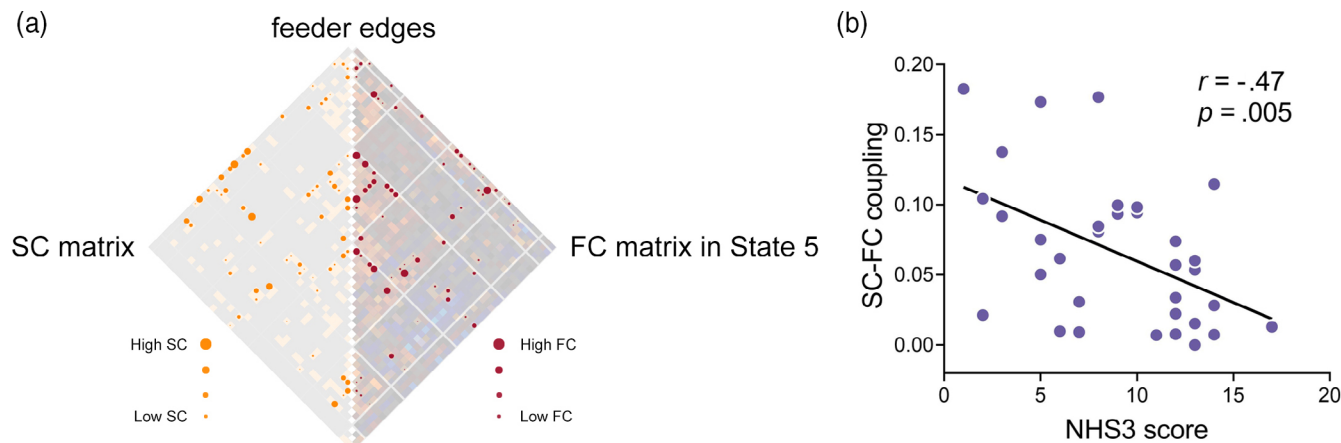


**FIGURE 6** Clinical association analysis. (a) Matrix representation of feeder edges in group-averaged structural connectivity (SC) and functional connectivity (FC) matrices. (b) Scatter plot showing the association between SC-FC coupling of feeder edges in State 5 and the National Hospital Seizure Severity Scale (NHS3) score in patients with juvenile myoclonic epilepsy (JME)

SC-FC coupling alterations in patients with JME. These results suggest the rich-club disorganization and its disrupted role in dynamic structure-function coupling for patients with JME at the early phase of the disease.

Patients with JME were found to exhibit weaker strength in anatomical rich-club edges than healthy controls. Studies examining structural brain network abnormalities in JME have provided evidence of white matter fiber changes in the corpus callosum, longitudinal fasciculus, and thalamic radiation (Ekmekci, Bulut, Gumustas, Yildirim, & Kustepe, 2016; Lee & Park, 2019; O'Muircheartaigh et al., 2012; Vollmar et al., 2012), and these track pathways often pass through the rich-club hubs we identified. It has been suggested that the connections among rich-club hubs form a central high-cost, high-capacity backbone for global brain communication (van den Heuvel et al., 2012). Thus, the SC reductions we observed may suggest a selective influence of the key pathways within this concentrated backbone rather than an equal effect of all connections among brain regions in JME. More importantly, we examined the impairment of rich-club organization in a cohort of treatment-naïve newly diagnosed patients, which reduced the potential influences of medication and chronic disease on our findings. Contemporary theories have suggested that JME is likely to be a neurodevelopmental condition (Wandschneider et al., 2019). Indeed, the myelination in highly connected fronto-parietal hubs has been demonstrated to continue post-natally until the third decade of life (Silbereis, Pochareddy, Zhu, Li, & Sestan, 2016), which overlaps with the frequent period of JME onset. Therefore, our current study suggests that atypical myelination in microstructure content may transform into changes in large-scale white matter connections among rich-club hubs which, in turn, lead to aberrant neurodevelopment of JME patient.

Studies on resting-state fMRI data have frequently revealed dynamic FC changes in patients with generalized epilepsy, ranging from individual connectivity circuit to network topologic organization (Liao et al., 2014; F. Liu et al., 2017; Zhang et al., 2018). Intriguingly, our results demonstrated significant group differences in FC

counterparts of structural connection categories in two distinct dynamic states including State 1 and State 5. As noted above, State 1 was characterized by the predominance of within-RSN connections, representing a functional segregation state. Abnormal FC within multiple RSNs, such as the sensorimotor, basal ganglia, executive control, and default mode networks, has been identified in previous studies of JME (Dong et al., 2016; Gleichgerrcht, Kocher, & Bonilha, 2015; Lee & Park, 2019; O'Muircheartaigh et al., 2012; Zhong et al., 2018). The reduced FC in State 1 demonstrated a wide RSNs dysfunction that may lead to various cognitive impairments in working memory, attention, and self-referential processing in patients with JME. Aside from dysconnectivity within RSNs, abnormal functional interaction between the insula (a key node of the CC) and motor system in patients with JME were also reported (Jiang et al., 2016; Paulus et al., 2015). Consequently, our lower FC in State 5, which had stronger positive connectivity between SM and CC, may suggest declined ability to integrate neural information between motor and cognitive control communities in JME. Furthermore, we observed that the SC-FC coupling of feeder edges in patients was decreased in both of the two abovementioned states. It is believed that the SC-FC coupling plays a critical role for developing higher-order executive functions such as working memory, mental flexibility, and inhibitory control (Misić et al., 2016; Vazquez-Rodriguez et al., 2019). Previous studies linking structural and static functional connectivity networks have indicated that people with epilepsy had lower SC-FC coupling both in the individual connection level and the whole brain level (Chiang, Stern, Engel Jr., & Haneef, 2015; Zhang et al., 2011). The present study extends current research to temporal dynamic domain and further suggests that attenuated structural support for functional communication may be dominated by distinct dynamic states, which in turn leads to different cognitive deficits in patients. Also, previous studies have reported that the SC-FC coupling is continuously remodeled with age in childhood and adolescence (Baum et al., 2020; Osmanlioglu et al., 2019), and this neurodevelopmental trajectory seems to be altered by various neuropsychiatric disorders (Collin

et al., 2017; Straathof, Sinke, Dijkhuizen, & Otte, 2019). Thus, our findings of state-specific coupling reductions may further suggest an abnormal reorganization in functional dynamics of structural topological properties during brain development, which may be prominently associated with failures of executive function observed in people with JME. More importantly, we found that the lower level of SC–FC coupling in State 5 was linked to greater disease severity. This finding is consistent with previous observations of associations between SC–FC decoupling and duration of epilepsy in patients (Chiang et al., 2015; Zhang et al., 2011), indicating that the early identified abnormalities in structure–function relationship may be implicated in the progress of the disease, and can be an indication of disrupted developmental processes in JME.

One important question concerns how structure–function coupling is related to the information transfer in dynamic functional networks for patients with JME. Extending the findings of time-invariant FC studies in generalized epilepsy (Liao et al., 2013; Pegg, Taylor, Keller, & Mohanraj, 2020; Pegg, Taylor, Laiou, Richardson, & Mohanraj, 2021), our patients showed lower global and local efficiencies in two dynamic connectivity patterns (i.e., State 1 and State 5), suggesting an inefficient brain information transfer in JME. We further observed the relationships between SC–FC coupling and functional network efficiency. Intriguingly, the SC–FC coupling of rich-club edges showed negative correlations with global and local efficiencies in State 1 for healthy controls, but these relationships were not significant for the patients, suggesting that the efficiency of brain information transfer in JME is no longer tethered by anatomical constraints on functional communication. Tightly coupled structure and function of hub regions have been demonstrated to support efficient communication among strongly interconnected association areas within segregated RSNs (Baum et al., 2020). At the same time, high SC–FC coupling in the key hubs could reduce competitive interference between different RSNs, allowing for the suppression of irrelevant cognitive activity while processing target brain information (Hampson, Driesen, Roth, Gore, & Constable, 2010). Therefore, the untethered relationships between SC–FC coupling and functional network efficiency in State 1 may suggest a reduced functional specialization of neural networks in patients with JME, paralleled by an inefficient functional flexibility and dynamic recruitment to balance various cognitive activities that are related to different RSNs, providing new evidence for the aberrant brain networks in this disease.

Our study has some limitations that should be noted. First, accurately reconstructing cortico-cortical white matter pathways from diffusion MRI remains challenging. In this study, we adopt a computationally inexpensive deterministic tractography to construct structural networks (Mori et al., 1999). It is well known that DTI has difficulty in detecting crossing fiber bundles, which may hinder the tracking algorithm from correctly tracing fiber streamlines (Jones, Knösche, & Turner, 2013), resulting in an underrepresentation of the number of connections of the structural network with reduced connectome sensitivity. Therefore, it would be important to see future attempts utilizing probabilistic tractography which is

advantageous in overcoming the fiber crossing problem to reconstruct white matter fiber pathways (Behrens, Johansen Berg, Jbabdi, Rushworth, & Woolrich, 2007). Second, epileptic transients have been suggested to influence resting-state functional connectivity (Bettus et al., 2011). Because it is difficult for patients to continue not to move their head, we did not record EEG data during MRI scanning in this study. It would be necessary to examine the effects of interictal epileptic discharges on SC–FC coupling in the future simultaneous EEG–fMRI study. Third, we mainly focused on the connections with nonzero structural connectivity when analyzing SC–FC coupling in our study, ignoring to consider the associations between FC and indirect fiber pathway. Previous studies have suggested that a strong FC could exist between regions with indirect SC (Honey et al., 2009). Future work should be done to assess the communicability for each structural network connection, which could capture the communication capacity through both direct and indirect SC between each pair of brain regions.

## 5 | CONCLUSIONS

Our study described the alterations of anatomical rich-club organization and abnormalities of dynamic SC–FC coupling in treatment-naïve newly diagnosed JME. SC differences in the patients versus healthy controls were in particular shown with connections among rich-club hubs. Moreover, the reduced SC–FC coupling of feeder edges in a strong SM–CC interaction state could reflect disease severity of patients JME with. Additionally, the global and local efficiencies of dynamic functional brain networks were decreased in patients, accompanied with a relaxed relationships between SC–FC coupling and network efficiency in a functional segregated state. Overall, these findings demonstrate a significant disruption of rich-club organization and altered role in dynamic structure–function coupling at the early stages of JME, which may contribute to the cognitive deficits such as impaired executive function in patients during development, advancing our understanding of the neurobiology mechanisms for this disorder.

## ACKNOWLEDGMENTS

The authors thank all participants in this study and also thank Lingshan Huang for English language help. This work was supported by the National Natural Science Foundation of China (No. 82160326, 61966023, 81801785, and 82172056), by the “Hundred Talents Program” of Zhejiang University, by the Fundamental Research Funds for the Central Universities (No. 2020FZZX001-05), by the Zhejiang Lab (No. 2019KE0AD01), by the China Postdoctoral Science Foundation (No. 2020M681865 and 2202M671727), by the Gansu Province Universities and Colleges Scientific Research Project (No. 2018A-124), and by the Cuiying Scientific and Technological Innovation Program of Lanzhou University Second Hospital (No. CY2018-QN03).

## CONFLICT OF INTEREST

The authors declare no competing interests.

## AUTHOR CONTRIBUTIONS

Guangyao Liu designed the study, performed the MRI data acquisition and the neuropsychological assessment, statistical analyses, drafted the manuscript, and approved the final manuscript as submitted. Weihao Zheng performed statistical analyses, drafted the manuscript, and approved the final manuscript as submitted. Hong Liu, Man Guo, Laiyang Ma, Wanjun Hu, and Ming Ke coordinated and carried out the data collection, revised the manuscript, and approved the final manuscript as submitted. Yu Sun and Jing Zhang critically reviewed the manuscript, and approved the final manuscript as submitted. Zhe Zhang conceptualized the study, drafted the manuscript, and approved the final manuscript as submitted.

## DATA AVAILABILITY STATEMENT

The data that support the findings of this study are available from the corresponding author (Z. Zhang) upon reasonable request.

## ORCID

Guangyao Liu  <https://orcid.org/0000-0003-0121-7001>

Weihao Zheng  <https://orcid.org/0000-0003-2996-5909>

Yu Sun  <https://orcid.org/0000-0002-6666-8586>

Zhe Zhang  <https://orcid.org/0000-0002-2725-4014>

## REFERENCES

- Allen, E. A., Damaraju, E., Plis, S. M., Erhardt, E. B., Eichele, T., & Calhoun, V. D. (2014). Tracking whole-brain connectivity dynamics in the resting state. *Cerebral Cortex*, 24(3), 663–676. <https://doi.org/10.1093/cercor/bhs352>
- Baum, G. L., Cui, Z., Roalf, D. R., Ciric, R., Betzel, R. F., Larsen, B., ... Satterthwaite, T. D. (2020). Development of structure–function coupling in human brain networks during youth. *Proceedings of the National Academy of Sciences of the United States of America*, 117(1), 771–778. <https://doi.org/10.1073/pnas.1912034117>
- Behrens, T. E. J., Johansen Berg, H., Jbabdi, S., Rushworth, M. F. S., & Woolrich, M. W. (2007). Probabilistic diffusion tractography with multiple fibre orientations: What can we gain? *NeuroImage*, 34(1), 144–155.
- Bell, A. J., & Sejnowski, T. J. (1995). An information-maximization approach to blind separation and blind deconvolution. *Neural Computation*, 7(6), 1129–1159.
- Bettus, G., Ranjeva, J. P., Wendling, F., Bénar, C. G., Confortgouny, S., Régis, J., ... Guye, M. (2011). Interictal functional connectivity of human epileptic networks assessed by intracerebral eeg and bold signal fluctuations. *PLoS One*, 6(5), e20071. <https://doi.org/10.1371/journal.pone.0020071.g001>
- Caeyenberghs, K., Powell, H. W., Thomas, R. H., Brindley, L., Church, C., Evans, J., ... Hamandi, K. (2015). Hyperconnectivity in juvenile myoclonic epilepsy: A network analysis. *NeuroImage: Clinical*, 7, 98–104. <https://doi.org/10.1016/j.nicl.2014.11.018>
- Calhoun, V. D., & Adali, T. (2016). Time-varying brain connectivity in fmri data: Whole-brain data-driven approaches for capturing and characterizing dynamic states. *IEEE Signal Processing Magazine*, 33(3), 52–66. <https://doi.org/10.1109/MSP.2015.2478915>
- Calhoun, V. D., Miller, R., Pearson, G., & Adali, T. (2014). The chronnectome: Time-varying connectivity networks as the next frontier in fmri data discovery. *Neuron*, 84(2), 262–274. <https://doi.org/10.1016/j.neuron.2014.10.015>
- Camfield, C. S., Striano, P., & Camfield, P. R. (2013). Epidemiology of juvenile myoclonic epilepsy. *Epilepsy & Behavior*, 28(Suppl 1), S15–S17. <https://doi.org/10.1016/j.yebeh.2012.06.024>
- Carvalho, K. C., Uchida, C. G., Guaranha, M. S., Guilhoto, L. M., Wolf, P., & Yacubian, E. M. (2016). Cognitive performance in juvenile myoclonic epilepsy patients with specific endophenotypes. *Seizure*, 40, 33–41. <https://doi.org/10.1016/j.seizure.2016.06.002>
- Chiang, S., Stern, J. M., Engel, J., Jr., & Haneef, Z. (2015). Structural-functional coupling changes in temporal lobe epilepsy. *Brain Research*, 1616, 45–57. <https://doi.org/10.1016/j.brainres.2015.04.052>
- Collin, G., Scholtens, L. H., Kahn, R. S., Hillegers, M. H. J., & van den Heuvel, M. P. (2017). Affected anatomical rich club and structural-functional coupling in young offspring of schizophrenia and bipolar disorder patients. *Biological Psychiatry*, 82(10), 746–755. <https://doi.org/10.1016/j.biopsych.2017.06.013>
- Cui, Z., Zhong, S., Xu, P., He, Y., & Gong, G. (2013). PANDA: A pipeline toolbox for analyzing brain diffusion images. *Frontiers in Human Neuroscience*, 7, 42. <https://doi.org/10.3389/fnhum.2013.00042>
- Damaraju, E., Allen, E. A., Belger, A., Ford, J. M., McEwen, S., Mathalon, D. H., ... Calhoun, V. D. (2014). Dynamic functional connectivity analysis reveals transient states of dysconnectivity in schizophrenia. *NeuroImage: Clinical*, 5, 298–308. <https://doi.org/10.1016/j.nicl.2014.07.003>
- Dong, L., Luo, C., Zhu, Y., Hou, C., Jiang, S., Wang, P., ... Yao, D. (2016). Complex discharge-affecting networks in juvenile myoclonic epilepsy: A simultaneous EEG-fMRI study. *Human Brain Mapping*, 37(10), 3515–3529. <https://doi.org/10.1002/hbm.23256>
- Ekmekci, B., Bulut, H. T., Gumustas, F., Yildirim, A., & Kustepe, A. (2016). The relationship between white matter abnormalities and cognitive functions in new-onset juvenile myoclonic epilepsy. *Epilepsy & Behavior*, 62, 166–170. <https://doi.org/10.1016/j.yebeh.2016.07.015>
- Fiorenzato, E., Strafella, A. P., Kim, J., Schifano, R., Weis, L., Antonini, A., & Biundo, R. (2019). Dynamic functional connectivity changes associated with dementia in Parkinson's disease. *Brain*, 142(9), 2860–2872. <https://doi.org/10.1093/brain/awz192>
- Gleichgerrcht, E., Kocher, M., & Bonilha, L. (2015). Connectomics and graph theory analyses: Novel insights into network abnormalities in epilepsy. *Epilepsia*, 56(11), 1660–1668. <https://doi.org/10.1111/epi.13133>
- Grayson, D. S., Ray, S., Carpenter, S., Iyer, S., Dias, T. G., Stevens, C., ... Fair, D. A. (2014). Structural and functional rich club organization of the brain in children and adults. *PLoS One*, 9(2), e88297. <https://doi.org/10.1371/journal.pone.0088297>
- Hampson, M., Driesen, N., Roth, J. K., Gore, J. C., & Constable, R. T. (2010). Functional connectivity between task-positive and task-negative brain areas and its relation to working memory performance. *Magnetic Resonance Imaging*, 28(8), 1051–1057. <https://doi.org/10.1016/j.mri.2010.03.021>
- Honey, C. J., Sporns, O., Cammoun, L., Gigandet, X., Thiran, J. P., Meuli, R., & Hagmann, P. (2009). Predicting human resting-state functional connectivity from structural connectivity. *Proceedings of the National Academy of Sciences of the United States of America*, 106(6), 2035–2040. <https://doi.org/10.1073/pnas.0811168106>
- Jerome Engel, J. (2001). A proposed diagnostic scheme for people with epileptic seizures and with epilepsy: Report of the ilae task force on classification and terminology. *Epilepsia*, 42(6), 796–803. <https://doi.org/10.1046/j.1528-1157.2001.10401.x>
- Jia, X., Ma, S., Jiang, S., Sun, H., Dong, D., Chang, X., ... Luo, C. (2018). Disrupted coupling between the spontaneous fluctuation and functional connectivity in idiopathic generalized epilepsy. *Frontiers in Neurology*, 9, 838. <https://doi.org/10.3389/fneur.2018.00838>
- Jiang, S., Luo, C., Gong, J., Peng, R., Ma, S., Tan, S., ... Yao, D. (2018). Aberrant thalamocortical connectivity in juvenile myoclonic epilepsy. *International Journal of Neural Systems*, 28(1), 1750034. <https://doi.org/10.1142/s0129065717500344>
- Jiang, S., Luo, C., Liu, Z., Hou, C., Wang, P., Dong, L., ... Yao, D. (2016). Altered local spontaneous brain activity in juvenile myoclonic epilepsy: A preliminary resting-state fMRI study. *Neural Plasticity*, 2016, 3547203. <https://doi.org/10.1155/2016/3547203>

- Jones, D. K., Knsche, T. R., & Turner, R. (2013). White matter integrity, fiber count, and other fallacies: The do's and don'ts of diffusion MRI. *NeuroImage*, 73, 239–254.
- Keown, C. L., Datko, M. C., Chen, C. P., Maximo, J. O., Jahedi, A., & Muller, R. A. (2017). Network organization is globally atypical in autism: A graph theory study of intrinsic functional connectivity. *Biological Psychiatry: Cognitive Neuroscience and Neuroimaging*, 2(1), 66–75. <https://doi.org/10.1016/j.bpsc.2016.07.008>
- Lee, H. J., & Park, K. M. (2019). Structural and functional connectivity in newly diagnosed juvenile myoclonic epilepsy. *Acta Neurologica Scandinavica*, 139(5), 469–475. <https://doi.org/10.1111/ane.13079>
- Li, R., Liao, W., Li, Y., Yu, Y., Zhang, Z., Lu, G., & Chen, H. (2016). Disrupted structural and functional rich club organization of the brain connectome in patients with generalized tonic-clonic seizure. *Human Brain Mapping*, 37(12), 4487–4499. <https://doi.org/10.1002/hbm.23323>
- Liao, W., Zhang, Z., Mantini, D., Xu, Q., Ji, G. J., Zhang, H., ... Lu, G. (2014). Dynamical intrinsic functional architecture of the brain during absence seizures. *Brain Structure & Function*, 219(6), 2001–2015. <https://doi.org/10.1007/s00429-013-0619-2>
- Liao, W., Zhang, Z., Mantini, D., Xu, Q., Wang, Z., Chen, G., ... Lu, G. (2013). Relationship between large-scale functional and structural covariance networks in idiopathic generalized epilepsy. *Brain Connectivity*, 3(3), 240–254. <https://doi.org/10.1089/brain.2012.0132>
- Liu, F., Wang, Y., Li, M., Wang, W., Li, R., Zhang, Z., ... Chen, H. (2017). Dynamic functional network connectivity in idiopathic generalized epilepsy with generalized tonic-clonic seizure. *Human Brain Mapping*, 38(2), 957–973. <https://doi.org/10.1002/hbm.23430>
- Liu, X., He, C., Fan, D., Zang, F., Zhu, Y., Zhang, H., ... Xie, C. (2021). Alterations of core structural network connectome associated with suicidal ideation in major depressive disorder patients. *Translational Psychiatry*, 11(1), 1–11. <https://doi.org/10.1038/s41398-021-01353-3>
- Misic, B., Betzel, R. F., de Reus, M. A., van den Heuvel, M. P., Berman, M. G., McIntosh, A. R., & Sporns, O. (2016). Network-level structure-function relationships in human neocortex. *Cerebral Cortex*, 26(7), 3285–3296. <https://doi.org/10.1093/cercor/bhw089>
- Mori, S., Crain, B. J., Chacko, V. P., & Van Zijl, P. C. (1999). Three-dimensional tracking of axonal projections in the brain by magnetic resonance imaging. *Annals of Neurology*, 45, 265–269.
- O'Muircheartaigh, J., Vollmar, C., Barker, G. J., Kumari, V., Symms, M. R., Thompson, P., ... Richardson, M. P. (2012). Abnormal thalamocortical structural and functional connectivity in juvenile myoclonic epilepsy. *Brain*, 135, 3635–3644. <https://doi.org/10.1093/brain/aws296>
- O'Donoghue, M. F., Duncan, J. S., & Sander, J. W. A. S. (1996). The National Hospital Seizure Severity Scale: A further development of the Chalfont seizure severity scale. *Epilepsia*, 37(6), 563–571.
- Osmanlioglu, Y., Tunc, B., Parker, D., Elliott, M. A., Baum, G. L., Ciric, R., ... Verma, R. (2019). System-level matching of structural and functional connectomes in the human brain. *NeuroImage*, 199, 93–104. <https://doi.org/10.1016/j.neuroimage.2019.05.064>
- Parsons, N., Bowden, S. C., Vogrin, S., & D'Souza, W. J. (2020). Default mode network dysfunction in idiopathic generalised epilepsy. *Epilepsy Research*, 159, 106254. <https://doi.org/10.1016/j.eplepsyres.2019.106254>
- Pascalichio, T. F., de Araujo Filho, G. M., da Silva Noffs, M. H., Lin, K., Caboclo, L. O., Vidal-Dourado, M., ... Yacubian, E. M. (2007). Neuropsychological profile of patients with juvenile myoclonic epilepsy: A controlled study of 50 patients. *Epilepsy & Behavior*, 10(2), 263–267. <https://doi.org/10.1016/j.yebeh.2006.11.012>
- Paulus, F. M., Krach, S., Blanke, M., Roth, C., Belke, M., Sommer, J., ... Knake, S. (2015). Fronto-insula network activity explains emotional dysfunctions in juvenile myoclonic epilepsy: Combined evidence from pupillometry and fMRI. *Cortex*, 65, 219–231. <https://doi.org/10.1016/j.cortex.2015.01.018>
- Pegg, E. J., Taylor, J. R., Keller, S. S., & Mohanraj, R. (2020). Interictal structural and functional connectivity in idiopathic generalized epilepsy: A systematic review of graph theoretical studies. *Epilepsy & Behavior*, 106(107), 13. <https://doi.org/10.1016/j.yebeh.2020.107013>
- Pegg, E. J., Taylor, J. R., Laiou, P., Richardson, M., & Mohanraj, R. (2021). Interictal electroencephalographic functional network topology in drug-resistant and well-controlled idiopathic generalized epilepsy. *Epilepsia*, 62(2), 492–503. <https://doi.org/10.1111/epi.16811>
- Ray, S., Miller, M., Karalunas, S., Robertson, C., Grayson, D. S., Cary, R. P., ... Fair, D. A. (2014). Structural and functional connectivity of the human brain in autism spectrum disorders and attention-deficit/hyperactivity disorder: A rich club-organization study. *Human Brain Mapping*, 35(12), 6032–6048. <https://doi.org/10.1002/hbm.22603>
- Sarwar, T., Ramamohanarao, K., & Zalesky, A. (2019). Mapping connectomes with diffusion MRI: Deterministic or probabilistic tractography? *Magnetic Resonance in Medicine*, 81(2), 1368–1384. <https://doi.org/10.1002/mrm.27471>
- Scheffer, I. E., Berkovic, S., Capovilla, G., Connolly, M. B., French, J., Guilhoto, L., ... Zuberi, S. M. (2017). ILAE classification of the epilepsies: Position paper of the ILAE Commission for Classification and Terminology. *Epilepsia*, 58(4), 512–521. <https://doi.org/10.1111/epi.13709>
- Silbereis, J. C., Pochareddy, S., Zhu, Y., Li, M., & Sestan, N. (2016). The cellular and molecular landscapes of the developing human central nervous system. *Neuron*, 89(2), 248–268. <https://doi.org/10.1016/j.neuron.2015.12.008>
- Smith, S. M., Miller, K. L., Salimi-Khorshidi, G., Webster, M., Beckmann, C. F., Nichols, T. E., ... Woolrich, M. W. (2011). Network modelling methods for FMRI. *NeuroImage*, 54(2), 875–891. <https://doi.org/10.1016/j.neuroimage.2010.08.063>
- Straathof, M., Sinke, M. R., Dijkhuizen, R. M., & Otte, W. M. (2019). A systematic review on the quantitative relationship between structural and functional network connectivity strength in mammalian brains. *Journal of Cerebral Blood Flow and Metabolism*, 39(2), 189–209. <https://doi.org/10.1177/0271678X18809547>
- Suarez, L. E., Markello, R. D., Betzel, R. F., & Misic, B. (2020). Linking structure and function in macroscale brain networks. *Trends in Cognitive Sciences*, 24(4), 302–315. <https://doi.org/10.1016/j.tics.2020.01.008>
- Sun, Y., Collinson, S. L., Suckling, J., & Sim, K. (2019). Dynamic reorganization of functional connectivity reveals abnormal temporal efficiency in schizophrenia. *Schizophrenia Bulletin*, 45(3), 659–669. <https://doi.org/10.1093/schbul/sby077>
- Tu, Y., Fu, Z., Mao, C., Falahpour, M., Gollub, R. L., Park, J., ... Kong, J. (2020). Distinct thalamocortical network dynamics are associated with the pathophysiology of chronic low back pain. *Nature Communications*, 11(1), 3948. <https://doi.org/10.1038/s41467-020-17788-z>
- Tu, Y., Fu, Z., Zeng, F., Maleki, N., Lan, L., Li, Z., ... Kong, J. (2019). Abnormal thalamocortical network dynamics in migraine. *Neurology*, 92(23), e2706–e2716. <https://doi.org/10.1212/WNL.0000000000007607>
- Ur Ozcelik, E., Kurt, E., Sirin, N. G., Eryurek, K., Ulasoglu Yildiz, C., Hari, E., ... Baykan, B. (2021). Functional connectivity disturbances of ascending reticular activating system and posterior thalamus in juvenile myoclonic epilepsy in relation with photosensitivity: A resting-state fMRI study. *Epilepsy Research*, 171(106), 569. <https://doi.org/10.1016/j.eplepsyres.2021.106569>
- van den Heuvel, M. P., Kahn, R. S., Goni, J., & Sporns, O. (2012). High-cost, high-capacity backbone for global brain communication. *Proceedings of the National Academy of Sciences of the United States of America*, 109(28), 11372–11377. <https://doi.org/10.1073/pnas.1203593109>
- van den Heuvel, M. P., & Sporns, O. (2011). Rich-club organization of the human connectome. *The Journal of Neuroscience*, 31(44), 15775–15786. <https://doi.org/10.1523/JNEUROSCI.3539-11.2011>
- van den Heuvel, M. P., Sporns, O., Collin, G., Scheewe, T., Mandl, R. C., Cahn, W., ... Kahn, R. S. (2013). Abnormal rich club organization and

- functional brain dynamics in schizophrenia. *JAMA Psychiatry*, 70(8), 783–792. <https://doi.org/10.1001/jamapsychiatry.2013.1328>
- Vazquez-Rodriguez, B., Suarez, L. E., Markello, R. D., Shafiei, G., Paquola, C., Hagmann, P., ... Misisic, B. (2019). Gradients of structure–function tethering across neocortex. *Proceedings of the National Academy of Sciences of the United States of America*, 116(42), 21219–21227. <https://doi.org/10.1073/pnas.1903403116>
- Vollmar, C., O'Muircheartaigh, J., Symms, M. R., Barker, G. J., Thompson, P., Kumari, V., ... Koepp, M. J. (2012). Altered microstructural connectivity in juvenile myoclonic epilepsy the missing link. *Neurology*, 78(20), 1555–1559. <https://doi.org/10.1212/WNL.0b013e3182563b44>
- Wandschneider, B., Hong, S. J., Bernhardt, B. C., Fadaie, F., Vollmar, C., Koepp, M. J., ... Bernasconi, A. (2019). Developmental MRI markers cosegregate juvenile patients with myoclonic epilepsy and their healthy siblings. *Neurology*, 93(13), e1272–e1280. <https://doi.org/10.1212/WNL.00000000000008173>
- Wandschneider, B., Thompson, P. J., Vollmar, C., & Koepp, M. J. (2012). Frontal lobe function and structure in juvenile myoclonic epilepsy: A comprehensive review of neuropsychological and imaging data. *Epilepsia*, 53(12), 2091–2098. <https://doi.org/10.1111/epi.12003>
- Wang, Y., Berglund, I. S., Uppman, M., & Li, T.-Q. (2019). Juvenile myoclonic epilepsy has hyper dynamic functional connectivity in the dorsolateral frontal cortex. *NeuroImage: Clinical*, 21, 101604. <https://doi.org/10.1016/j.nicl.2018.11.014>
- Yan, C., & Zang, Y. (2010). DPARSF: A MATLAB toolbox for “pipeline” data analysis of resting-state fMRI. *Frontiers in Systems Neuroscience*, 4, 13. <https://doi.org/10.3389/fnsys.2010.00013>
- Yu, Q., Erhardt, E. B., Sui, J., Du, Y., He, H., Hjelm, D., ... Calhoun, V. D. (2015). Assessing dynamic brain graphs of time-varying connectivity in fMRI data: Application to healthy controls and patients with schizophrenia. *NeuroImage*, 107, 345–355. <https://doi.org/10.1016/j.neuroimage.2014.12.020>
- Zhang, Z., Liao, W., Chen, H., Mantini, D., Ding, J. R., Xu, Q., ... Lu, G. (2011). Altered functional-structural coupling of large-scale brain networks in idiopathic generalized epilepsy. *Brain*, 134(Pt 10), 2912–2928. <https://doi.org/10.1093/brain/awr223>
- Zhang, Z., Liu, G., Yao, Z., Zheng, W., Xie, Y., Hu, T., ... Hu, B. (2018). Changes in dynamics within and between resting-state subnetworks in juvenile myoclonic epilepsy occur at multiple frequency bands. *Frontiers in Neurology*, 9, 448. <https://doi.org/10.3389/fneur.2018.00448>
- Zhang, Z., Liu, G., Zheng, W., Shi, J., Liu, H., & Sun, Y. (2020). Altered dynamic effective connectivity of the default mode network in newly diagnosed drug-naïve juvenile myoclonic epilepsy. *NeuroImage: Clinical*, 28(102), 431. <https://doi.org/10.1016/j.nicl.2020.102431>
- Zhao, S., Wang, G., Yan, T., Xiang, J., Yu, X., Li, H., & Wang, B. (2020). Sex differences in anatomical rich-club and structural-functional coupling in the human brain network. *Cerebral Cortex*, 31, 1987–1997. <https://doi.org/10.1093/cercor/bhaa335>
- Zhong, C., Liu, R., Luo, C., Jiang, S., Dong, L., Peng, R., ... Wang, P. (2018). Altered structural and functional connectivity of juvenile myoclonic epilepsy: An fMRI study. *Neural Plasticity*, 2018, 1–12. <https://doi.org/10.1155/2018/7392187>

## SUPPORTING INFORMATION

Additional supporting information may be found in the online version of the article at the publisher's website.

**How to cite this article:** Liu, G., Zheng, W., Liu, H., Guo, M., Ma, L., Hu, W., Ke, M., Sun, Y., Zhang, J., & Zhang, Z. (2022). Aberrant dynamic structure–function relationship of rich-club organization in treatment-naïve newly diagnosed juvenile myoclonic epilepsy. *Human Brain Mapping*, 43(12), 3633–3645. <https://doi.org/10.1002/hbm.25873>